

PAPER • OPEN ACCESS

## Effect of the Coriolis force on the macrosegregation of aluminum in the centrifugal casting of Ti-Al alloys

To cite this article: M. Cisternas Fernández *et al* 2019 *IOP Conf. Ser.: Mater. Sci. Eng.* **529** 012033

View the [article online](#) for updates and enhancements.



**IOP | ebooks™**

Bringing you innovative digital publishing with leading voices to create your essential collection of books in STEM research.

Start exploring the collection - download the first chapter of every title for free.

# Effect of the Coriolis force on the macrosegregation of aluminum in the centrifugal casting of Ti-Al alloys

M. Cisternas Fernández<sup>1</sup>, M. Založnik<sup>1</sup>, H. Combeau<sup>1</sup>, C. Huang<sup>2</sup>, J. Zollinger<sup>1</sup> and U. Hecht<sup>2</sup>

<sup>1</sup> Université de Lorraine, CNRS, IJL, F-54000 Nancy, France

<sup>2</sup> Access e.V., Intzestr. 5, D-52072 Aachen, Germany

E-mail: martin.cisternas-fernandez@univ-lorraine.fr

**Abstract.** Within the framework of the ESA GRADECET project, experiments of directional solidification of cylindrical Ti-Al samples were conducted in hypergravity. The experiments were performed in a centrifuge with the apparent gravity (sum of centrifugal and terrestrial gravity) aligned along the cylinder centerline. 3D numerical simulations of aluminum macrosegregation in these samples are presented. A volume-averaging solidification model is used that accounts for centrifugal and Coriolis accelerations in a non-inertial rotating reference system. We compare the melt flow pattern and the macrosegregation formation under terrestrial gravity and under  $20g$  centrifugation. The results show that the Coriolis acceleration, although very weak, breaks the symmetry of the thermosolutal convection, having an important impact on the final macrosegregation pattern. The macrosegregation is entirely modified in comparison with a sample solidified under terrestrial gravity conditions. Besides the aluminum segregation intensity increases with the centrifugation level.

## 1. Introduction

Titanium aluminum alloys have been studied during the last 30 years due to their low density and high resistance in high temperature environments, making them a very good candidates for automotive and aerospace applications. However, their high reactivity in the liquid state makes them difficult to cast as they need to be cast at very low superheats and at fast filling rates. Centrifugal casting is a possibility to enhance the mold filling speed by combining the effect of terrestrial gravity and centrifugal acceleration, preventing undesired reactions and porosity defects.

In spite of the benefits of centrifugal casting, it can increase the magnitude of the liquid thermosolutal convection during solidification and consequently increase the segregation of alloying elements. In the case of Ti-Al alloys, controlling the macrosegregation of centrifugally cast ingots is important since the microstructure formation is very sensitive to the aluminum composition [1]. Solidification during centrifugation has been studied before. Ramachandran et al. [2] performed numerical simulations attempting to emulate the liquid thermally driven convection that takes place in a centrifuge-based Bridgman crystal growth configuration, reporting that the Coriolis acceleration played a stabilizing role in cases where the centrifugal acceleration was parallel to the thermal gradient. Experimental studies of solidification in centrifuges, such as the one of Rodot et al. [3] or Muller et al. [4] concluded that the Coriolis acceleration and centrifugal acceleration gradients can play an important role on liquid convection. Although



Coriolis acceleration is known to have an impact on the liquid convection during solidification, its effect on macrosegregation has not been studied yet.

The European Space Agency (ESA) launched the GRADECET (“GRAVity DEpendence of Columnar to Equiaxed Transition”) project, whose main objective is to investigate the influence of gravity on the Columnar-to-Equiaxed Transition - *CET* - and on microstructure formation in peritectic Ti-Al alloys. Within the framework of this project, several experiments of directional solidification in hypergravity were carried out on the ESA “Large Diameter Centrifuge” (LDC). These experiments gave relevant information on the solidification microstructure formed under different gravity levels [1]. To fully understand the experimental observations, characterization of the liquid thermosolutal convection during solidification is needed. This work aims to support the understanding of the liquid convection and of macrosegregation formation by means of numerical simulations.

We implemented a solidification model for columnar growth that takes into account the liquid thermosolutal convection considering the non-inertial accelerations - centrifugal and Coriolis - into the finite-volume framework OpenFOAM. We perform 3D numerical simulations of the GRADECET experiments for the alloy Ti-48Al-2Cr-2Nb and we show that the Coriolis acceleration has a large impact on the macrosegregation because it breaks the symmetry of the liquid convection, leading to an entirely three-dimensional aluminum segregation pattern.

## 2. The model

The volume-average solidification model is similar to the one used by Combeau et al. [5] and accounts for columnar growth with a fixed solid phase in a binary alloy. The momentum equation is defined in terms of the intrinsic average liquid velocity  $\langle \vec{v}_l \rangle^l$  and takes into account the centrifugal and Coriolis accelerations. The buoyancy term is modeled using a Boussinesq approximation which considers the thermal and solutal contributions. In addition, the energy equation is solved for the averaged enthalpy  $\langle h \rangle = c_p T + g_l L_f$ , where  $c_p$  is the specific heat,  $g_l$  the liquid fraction and  $L_f$  the latent heat. It is assumed that the temperature in the liquid is the same as in the solid  $T = T_l = T_s$ . Finally, a model assuming infinitely fast diffusion at the microscopic scale is used for the solid growth (lever rule). The equations of the model are:

- *Mass conservation:* Only the liquid movement is considered.

$$\nabla \cdot (g_l \langle \vec{v}_l \rangle^l) = 0 \quad (1)$$

- *Liquid momentum conservation:*

$$\begin{aligned} \frac{\partial}{\partial t} (g_l \langle \vec{v}_l \rangle^l) + \nabla \cdot (g_l \langle \vec{v}_l \rangle^l \langle \vec{v}_l \rangle^l) + 2g_l (\vec{\omega} \times \langle \vec{v}_l \rangle^l) = \\ - g_l \nabla p + \nabla \cdot (g_l \nu_l \nabla \langle \vec{v}_l \rangle^l) - \frac{\nu_l \rho g_l^2}{K} \langle \vec{v}_l \rangle^l + g_l \rho_l^b [\vec{g} - \vec{\omega} \times (\vec{\omega} \times \vec{x}_c)] \end{aligned} \quad (2)$$

Where  $\rho_l^b = \rho (1 - \beta_T (T - T_{ref}) - \beta_C (C_l - C_{ref}))$  and  $K = \frac{\lambda_{2g_l}^2 g_l^3}{180(1-g_l)^2}$

- *Energy conservation:*

$$\frac{\partial \langle h \rangle}{\partial t} + \nabla \cdot (g_l \langle \vec{v}_l \rangle^l h_l) - \frac{1}{\rho} \nabla \cdot (k \nabla T) = 0 \quad (3)$$

Where  $h_l = c_p T + L_f$

- *Solute conservation:* Macroscopic solute diffusion is neglected.

$$\frac{\partial \langle C \rangle}{\partial t} + \nabla \cdot (g_l \langle \vec{v}_l \rangle^l C_l) = 0 \quad (4)$$

- *Supplementary relations:*

- Averaged solute concentration:

$$\langle C \rangle = g_l C_l + g_s C_s \quad (5)$$

- Microsegregation model (infinitely fast microscopic diffusion):

$$T = T_f + m_l C_l \quad (6)$$

$$C_s = k_p C_l \quad (7)$$

The alloy with which the GRADECET experiments were performed undergoes a peritectic transformation in its solidification path near 1480 [°C] [6]. A simulation of the solidification path was performed using Thermo-Calc Software [7] considering full thermodynamic equilibrium between the phases. Figure 1 presents the averaged aluminum concentration in solid and liquid phases obtained with Thermo-Calc and the approximations for the *liquidus* and *solidus* lines used in this work. In addition, Figure 2 presents the corresponding solidification path that assumes thermodynamic equilibrium between all phases along with the solidification path used in this work. The simplified solidification path considers a pseudo-eutectic transformation at  $T = 1479.7[^\circ\text{C}]$ . Table 1 presents the list of thermophysical parameters that are used in the numerical simulations.

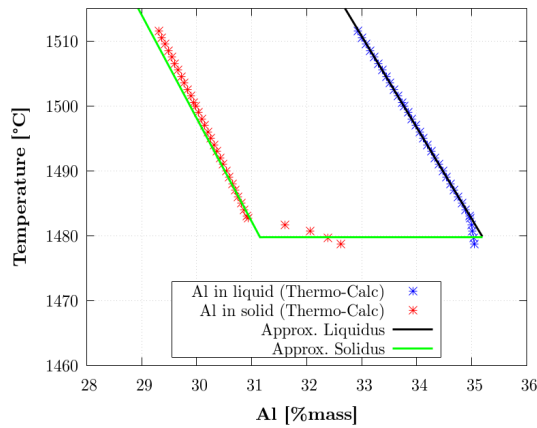


**Figure 1.** Averaged concentration of aluminum in the different phases vs temperature.

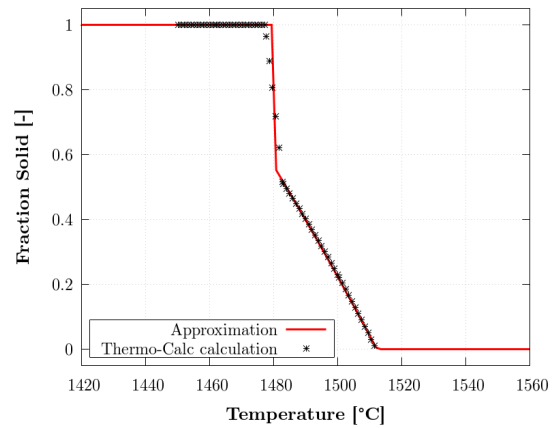


**Figure 2.** Solidification path obtained with Thermo-Calc Software and approximation used in the modeling.

### 3. Case study

The GRADECET experiments consisted of cylindrical Ti-Al samples (8 [mm] diameter, 165[mm] length) which were first remelted and then directionally solidified by means of a furnace that followed a specific thermal treatment to induce the *CET*. The furnace was mounted in the LDC and its thermal treatment was performed using three heaters located along the sample. The LDC centrifuge arm is 4[m] long, so that large centrifugal accelerations can be produced at relatively low rotational velocity. The furnace was free to tilt, such that the total apparent gravity  $\vec{g}_{tot}$  was aligned with the cylinder centerline.

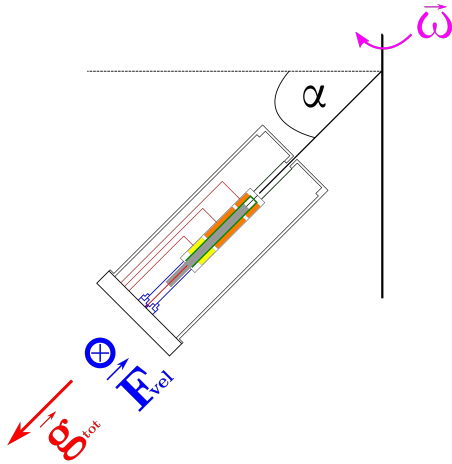
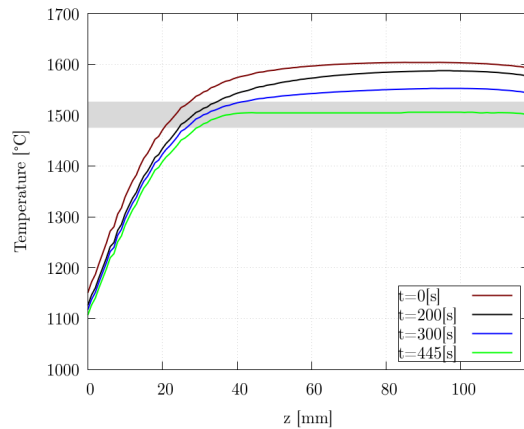
Figure 3 shows a schematic of the furnace in the centrifuge with the three heaters and the Ti-Al sample. The main plane of study is the one formed by the total apparent gravity  $\vec{g}_{tot}$

**Table 1.** Thermophysical properties used in the simulations.

Property	Symbol	Units	Value
Nominal aluminum concentration	$C_0$	[%mass]	32.96
Partition coefficient	$k_p$	[—]	0.885
Melting point of the pure substance	$T_f$	[°C]	1975.66
Liquidus slope	$m_l$	[°C/%mass]	-14.089
Pseudo-eutectic concentration	$C_{eut}$	[%mass]	35.2
Reference density	$\rho$	[kg/m <sup>3</sup> ]	3877.8
Kinematic viscosity	$\nu_l$	[m <sup>2</sup> /s]	$1.65 \times 10^{-6}$
Thermal conductivity	$k$	[W/m°C]	19.9
Solutal expansion coeff.	$\beta_C$	[%mass <sup>-1</sup> ]	$8.465 \times 10^{-3}$
Thermal expansion coeff.	$\beta_T$	[°C <sup>-1</sup> ]	$1.1785 \times 10^{-4}$
Latent heat	$L_f$	[J/kg]	$3.62 \times 10^5$
Secondary arm spacing	$\lambda_2$	[m]	$6.50 \times 10^{-5}$

and flight velocity  $\vec{F}_{vel}$  vectors (as shown in Fig. 3) since the effect of the Coriolis force is more comprehensive on it. Thermal boundary conditions at the surface of the Ti-Al sample were obtained by heat transfer simulations of the full furnace by a dedicated furnace model. The temperature evolution extracted from the thermal simulations was imposed as Dirichlet b.c. at the sample surface in the solidification simulations.

Numerical simulations of macrosegregation were performed considering one level of centrifugation, where the total apparent gravity (sum of centrifugal acceleration and terrestrial gravity) was  $20\vec{g}$  ( $\vec{g}$ : normal terrestrial gravity) and one simulation accounting only for terrestrial gravity (without centrifugation).

**Figure 3.** Schematic of the furnace and the sample in the centrifuge. Ti-Al sample (grey), heaters (yellow and orange) and thermocouples (red).**Figure 4.** Temperature boundary conditions on the cylinder surface at different times.

#### 4. Results and discussion

During solidification, the temperature gradient along the cylinder was anti-parallel to the total apparent gravity. With the onset of solidification, the cylinder side is slightly colder than its center due to the change of temperature in the heaters, so that, the first solid is formed at the cylinder side. Aluminum is rejected from the growing solid enriching the liquid in the mushy zone and thus decreasing its liquid density.

Figure 5 presents a comparison of the liquid flow between the cases 1G ( $\vec{g}_{tot} = 1\vec{g}$ ) and 20G ( $\vec{g}_{tot} = 20\vec{g}$ ) at  $t = 300[s]$  in the main plane of study. It can be observed that in the 1G case, the liquid flow is completely axisymmetric while in the 20G case, the Coriolis force, although very weak ( $\frac{2(\vec{\omega} \times \langle \vec{v}_l \rangle)^l}{\vec{g}_{tot}} \sim 10^{-4}$ ), entirely modifies the convection producing a three-dimensional fluid flow pattern. In the 1G case, the aluminum enriched liquid, that at the beginning is located in the cylinder sides, moves upward from the bottom of the mushy zone to the top entering to the fully liquid region. This aluminum enriched liquid advances along the cylinder by the cylinder side arriving to a point where the superheated liquid, that is lighter due to the thermal effect, blocks its advance. Finally, the liquid returns to the mushy zone by the cylinder centerline. On the other hand, in the 20G case, the Coriolis acceleration pushes the aluminum enriched liquid, that moves upward from the bottom of the mushy zone, to the flight velocity side of the cylinder. The lighter liquid flows from the mushy zone to the top of the cylinder by the flight velocity side and returns to the mushy zone by the opposite to flight velocity side. We found that the maximum liquid velocity in the 1G case is around 0.1[mm/s] while in the 20G case is 5[mm/s].

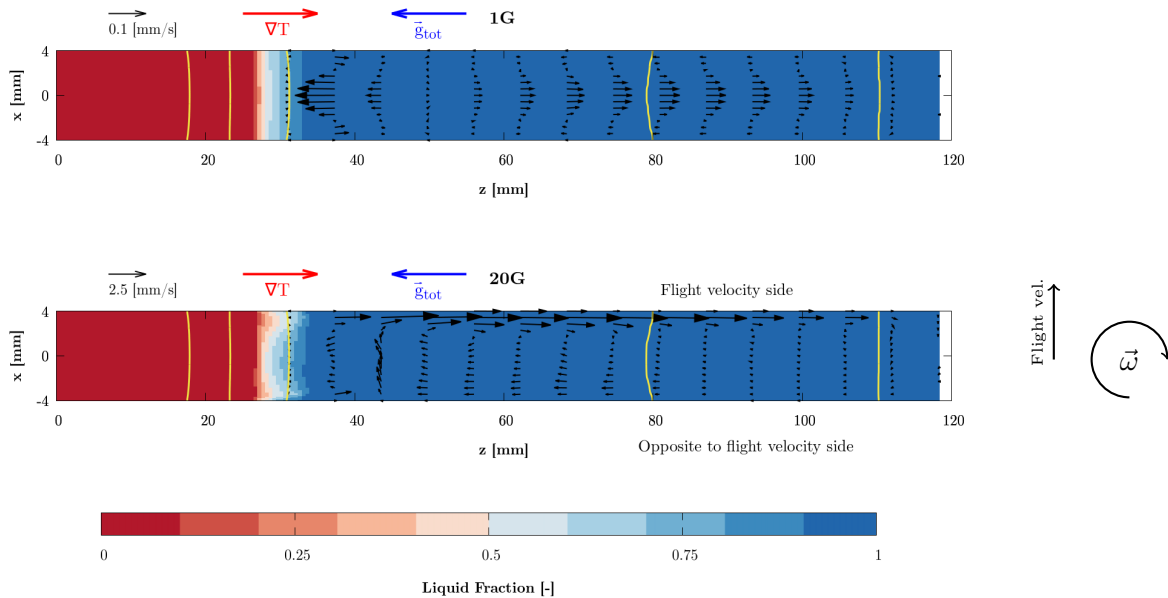


**Figure 5.** Comparison of the liquid convection between the 1G and 20G cases at  $t = 300[s]$ . Temperature contours in yellow from left to right: 1400,1450,1500,1550 [° C].

The three-dimensional thermosolutal driven flow advects the aluminum throughout the domain leading to macrosegregation. Figure 6 presents the aluminum segregation map in the main plane of study for the 1G and 20G cases. We can see that increasing the total apparent gravity, the segregation intensity is increased due to the stronger thermosolutal convection. The aluminum segregation in the 1G case is axisymmetric as well as its liquid motion while in the case with centrifugation, the flight velocity side of the sample is aluminum enriched. This segregation pattern follows the criterion  $\frac{\partial \langle C \rangle}{\partial t} \sim \langle \vec{v}_l \rangle^l \cdot \nabla T$  that can be obtained by combining Eqs. 1, 4 and

6.

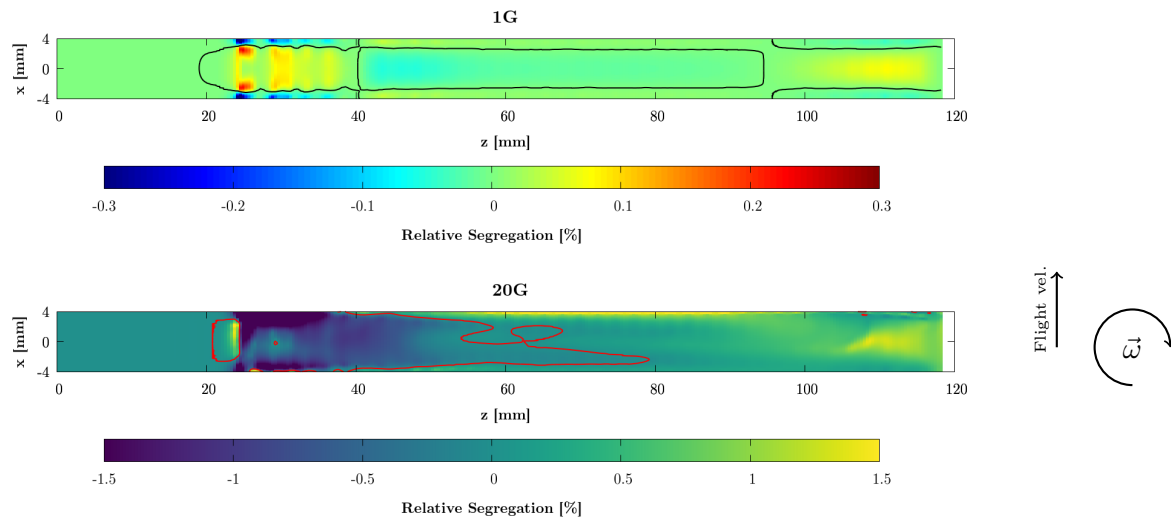


**Figure 6.** Aluminum segregation in the main plane at the end of solidification for the 1G and 20G cases. Relative Segregation:  $\frac{\langle C \rangle - C_0}{C_0} \times 100\%$ . Contours at  $\langle C \rangle = C_0$  (red line) separate the positively and negatively segregated zones.

## 5. Conclusions

The 3D numerical simulations of aluminum macrosegregation show that the impact of the Coriolis acceleration in centrifugally solidified Ti-Al samples is large although its magnitude is small compared to the centrifugal acceleration. The Coriolis acceleration breaks the symmetry of the flow structure compared to samples solidified under normal terrestrial gravity conditions and changes the pattern of aluminum segregation. Additionally, the centrifugation increases the aluminum segregation intensity.

## References

- [1] Reilly N 2016 *Hétérogénéités de fabrication des aluminiums de titane: caractérisation et maîtrise de leurs formations en coulée centrifuge* Ph.D. thesis Université de Lorraine
- [2] Ramachandran N, Downey J, Curreri P and Jones J 1993 *Journal of crystal growth* **126** 655–674
- [3] Rodot H, Regel L and Turtchaninov A 1990 *Journal of crystal growth* **104** 280–284
- [4] Müller G, Neumann G and Weber W 1992 *Journal of crystal growth* **119** 8–23
- [5] Combeau H, Bellet M, Fautrelle Y, Gobin D, Arquis E, Budenkova O, Dussoubs B, Du Terrail Y, Kumar A, Gandin C *et al.* 2012 Analysis of a numerical benchmark for columnar solidification of binary alloys *IOP Conference Series: Materials Science and Engineering* vol 33 (IOP Publishing)
- [6] Witusiewicz V, Bondar A, Hecht U, Rex S and Velikanova T Y 2008 *Journal of Alloys and Compounds* **1** 185–194
- [7] Andersson J O, Helander T, Höglund L, Shi P and Sundman B 2002 *Calphad* **26** 273–312

## Acknowledgments

This work was carried out as part of the GRADECET (GRAVity DEpendence of Columnar to Equiaxed Transition in TiAl Alloys) research project and was funded by the European Space Agency (contract 4000114221/15/NL/PG). The view expressed herein can in no way be taken to reflect the official opinion of the European Space Agency.